Biochemical and Biophysical Research Communications 486 (2017) 391–397

Contents lists available at ScienceDirect

Biochemical and Biophysical Research Communications

journal homepage: www.elsevier.com/locate/ybbrc

Sublethal doses of neonicotinoid imidacloprid can interact with honey bee chemosensory protein 1 (CSP1) and inhibit its function

Hongliang Li [a, *, 1], Jing Tan [a, 1], Xinmi Song [a], Fan Wu [a], Mingzhu Tang [a], Qiyun Hua [b], Huoqing Zheng [c], Fuliang Hu [c]

[a] Zhejiang Provincial Key Laboratory of Biometrology and Inspection & Quarantine, College of Life Sciences, China Jiliang University, Hangzhou 310018, PR China
[b] Jinhua Academy of Agricultural Science, Jinhua 321000, PR China
[c] College of Animal Sciences, Zhejiang University, Hangzhou 310058, PR China

ARTICLE INFO

Article history:
Received 26 February 2017
Accepted 13 March 2017
Available online 14 March 2017

Keywords:
Apis cerana
Chemosensory protein
Neonicotinoid imidacloprid
Binding interaction
Functional inhibition

ABSTRACT

As a frequently used neonicotinoid insecticide, imidacloprid can impair the chemoreceptive behavior of honey bees even at sublethal doses, while the physiochemical mechanism has not been further revealed. Here, multiple fluorescence spectra, thermodynamic method, and molecular docking were used to study the interaction and the functional inhibition of imidacloprid to the recombinant CSP1 protein in Asian honey bee, *Apis cerana*. The results showed that the fluorescence intensity ($\lambda_{em} = 332$ nm) of CSP1 could be significantly quenched by imidacloprid in a dynamic mode. During the quenching process, $\Delta H > 0$, $\Delta S > 0$, indicating that the acting forces of imidacloprid with CSP1 are mainly hydrophobic interactions. Synchronous fluorescence showed that the fluorescence of CSP1 was mainly derived from tryptophan, and the hydrophobicity of tryptophan decreased with the increase of imidacloprid concentration. Molecular docking predicted the optimal pose and the amino acid composition of the binding process. Circular dichroism (CD) spectra showed that imidacloprid reduced the α-helix of CSP1 and caused the extension of the CSP1 peptide chain. In addition, the binding of CSP1 to floral scent β-ionone was inhibited by nearly 50% of the apparent association constant (K_A) in the presence of 0.28–2.53 ng/bee of imidacloprid, and the inhibition rate of nearly 95% at 3.75 ng/bee of imidacloprid at sublethal dose level. This study initially revealed the molecular physiochemical mechanism that sublethal doses of neonicotinoid still interact and inhibit the physiological function of the honey bees' chemoreceptive system.

1. Introduction

In complex natural environment, insects rely on the acute chemical communication system to rapidly cognize and make response to the various kinds of semiochemicals existing in the surrounding [1]. In the insect chemoreceptive system, there are always two kinds of acidic and low molecular chemical communication related proteins, chemosensory proteins (CSPs) and odorant-binding proteins (OBPs) [2]. In general, CSPs and OBPs contain 4 and 6 conserved cysteines, respectively, forming two and three pairs of disulfide bonds. Typical OBPs are specifically expressed in olfactory organs such as antennae, and are associated with olfactory function; and CSPs are thought to be associated with chemoreceptive sense to chemical information. Because they were first found in insect chemosensory tissues, and are known as chemosensory proteins [3].

As one of the significant components of insect chemoreceptive system, CSPs are considered to have complex physiological functions, such as limb regeneration [4], embryonic development [5], and even behavioral changes [6], in addition to chemoreception towards semiochemicals. However, more and more reports have showed that CSPs exhibit similar olfactory function and characteristics as OBPs, such as in the case of *Adelphocoris* lineolatus [7,8], *Frankliniella occidentalis* [9], and *Bemisia tabaci* [10], CSPs participate in the identification of different parasitic plant volatiles, including repellent odors. Moreover, CSPs were also found to strongly bind the insect semiochemicals or pheromones, such as in *Schistocerca gregaria* [11], *Carausius morosus* [12], *Apis mellifera* [13], and *Camponotus japonicas* [14] and so on.

* Corresponding author.
E-mail address: atcjlu@126.com (H. Li).
[1] These authors contributed equally to this work.

http://dx.doi.org/10.1016/j.bbrc.2017.03.051
0006-291X/

Neonicotinoid insecticides, being the pesticide most widely used in the world in recent thirty years, can inhibit the bioactivity of the insect nicotinic type acetylcholine receptor as part of the nervous system of insects [15]. Although the neonicotinoid insecticides exhibit broad-spectrum systemic characteristics, high neurotoxicity of pests and low toxicity to humans and animals [16], they can be highly toxicant to some beneficial insects such as honey bees. For example, the mean acute oral toxicity (AOT) LD_{50} values of imidacloprid at 72 h is 69.68 ng/honey bee [17].

Recent more evidences have indicated that the exposure to field level pesticides can affect honey bees on learning performance, behavior, and neurophysiology, although they do not cause direct mortality (so called sublethal effect) [18]. While these sublethal doses do not kill individual bees, they may seriously influence on the activities and functioning of the whole bee colony [19,20]. Recently there have been some noteworthy reports that sublethal doses of insecticide treatment can dramatically cause changes in the transcriptional level of insect CSPs genes, such as the up-regulation of *CSP8* in the diamondback moth, *Plutella xylostella*, treated with permethrin [21], *CSP1* and *CSP2* in the silkworm, *Bombyx mori*, treated by avermectins [22], and *CSP1* in the whitefly, *Bemisia tabaci*, treated with neonicotinoid thiamethoxa [23]. These studies showed that insect CSPs seem to be able to respond to insecticides, while it remains still unknown whether the insecticides interact directly with CSPs, thus affecting their chemoreceptive functions.

The Asian honey bee, *Apis cerana*, has a sensitive developed sense of chemoreceptive and olfactory system to prefer the wide range of flowers, including wild plants [24]. In the previous study, the chemosensory protein CSP1 was found to be highly expressed in the antennae of worker honey bee, and had a strong affinity with natural semiochemicals such as β-ionone. It indicates that CSP1 is a typical chemoreceptive protein involved in the chemosensory system of *A. cerana* [25]. As the exposure to sublethal doses of neonicotinoid imidacloprid have been widely evidenced to impair chemoreceptive associative behavior involved in foraging, olfactory learning, memory and other advanced cognitive functions of worker honey bees [26–28], in this study, by means of the combined multiple fluorescence spectroscopy, thermodynamics and docking analysis, we first demonstrated the direct interaction between imidacloprid and CSP1 as well as the functional inhibition of CSP1 binding to natural semiochemical in vitro. The evidences initially not only elucidate the molecular basis of neonicotinoid insecticide at sublethal dose level affecting and impairing the chemoreceptive function of honey bee, *A. cerana*, but also provide a theoretical explanation for the chemoreceptive response of honey bees under sublethal neonicotinoid insecticide stress.

2. Materials and methods

2.1. Chemicals and reagents

Imidacloprid (>97% purity) (the chemical structure is shown in Fig. 1(A)) and β-ionone (>98% purity) were both purchased from TCI co. Japan, and dissolved in spectroscopic pure grade methanol (Tedia, USA) to prepare 1.0×10^{-3} mol L^{-1} stock solutions, and stored at 4 °C in the dark. Milli-Q water (18.2 MΩ, Millipore, US) was used throughout, and all the other solvents and chemicals used in this study were of analytical reagent grade.

2.2. Preparation of recombinant CSP1 protein

CSP1 gene was amplified by RT-PCR form worker bees antennae, then cloned into pMD18-T vector [29]. The *CSP1* gene was then cloned into pET-32a (+) vector and transformed into BL21 (DE3) competent cells for expression of CSP1 protein. After induction with the concentration of 1 mmol L^{-1} IPTG, the recombinant CSP1 protein was purified by affinity chromatography on a ProteinIso™ Ni^{2+}-NTA Resin column, and dialyzed by using PBS buffer (pH 7.4) for 72 h at 4 °C to obtain soluble recombinant CSP1 protein. The final concentration of CSP1 was measured by Bradford method, then quantified to be 1 μmol L^{-1}, and stored at −20 °C until use.

2.3. Multiple fluorescence spectra of CSP1 protein with imidacloprid

(1) Fluorescence quenching spectroscopy. Fluorescence quenching spectra were obtained by using RF-5301pc type fluorescence spectrophotometer (Shimadzu, JP). The fluorescence excitation wavelength is 281 nm, the fluorescence emission and excitation slit width is 5 nm, and the scanning range is 290–500 nm. The CSP1 recombinant protein was diluted to 1 μmol L^{-1} with PBS buffer (pH 7.4), and added to the quartz cuvette with 1 cm width. The CSP1 protein was continuously titrated by 1 mmol L^{-1} imidacloprid, and the fluorescence emission spectra of the protein were recorded until the maximum fluorescence intensity no longer decreased. The thermodynamic experimental temperatures were set at 284 K and 294 K, respectively.

(2) Synchronous fluorescence (SF) spectra. The SF spectra of tyrosine and tryptophan in CSP1 were recorded at $\Delta\lambda$ (λ_{ex} - λ_{em}) = 15 and 60 nm, respectively. The polarities change of the binding microenvironment were determined when imidacloprid binding to CSP1 protein.

(3) Ultraviolet absorption (UV) spectra. The UV spectra were obtained by using UV-1800 type UV-vis spectrophotometer (Shimadzu, JP). The UV spectra of CSP1 and the mixture of CSP1 and imidacloprid with equal ratio were measured at a wavelength of 190–400 nm.

2.4. Circular dichroism (CD) spectra

CSP1 was titrated with different concentrations of imidacloprid, and the CD spectra were scanned in the range of 200–250 nm. The molar ratio of protein to imidacloprid was 1: 0, 1: 0.5 and 1: 4, respectively. The secondary structure changes of CSP1 were calculated from the CD spectroscopic data by the SELCON3 program [30].

2.5. Molecular docking analysis

The interaction pattern between the protein and the small molecule ligand can be analyzed by molecular docking [31]. The predicted three-dimensional crystal structure of CSP1 was obtained based on the homologous prediction from *Mamestra brassicae* CSPMbraA6 crystal structure (PDB entry code, 1n8v) [32] via the SWISS-MODEL server [33]. The 3D structure of imidacloprid was obtained in NCBI (registration code: 638014). By using Molegro Virtual Docker (MVD) 4.2 software (beta trial), the imidacloprid was docked into the predicted binding cavity of CSP1 crystal structure. The search and scoring criteria of optimal binding poses were calculated and evaluated based on the MolDock Optimizer and MolDock Score, respectively [34].

2.6. Functional inhibition of CSP1 by imidacloprid

The 1 μmol L^{-1} CSP1 protein solution was titrated with 10 mmol L^{-1} β-ionone in the same method as in section 2.3-(1) above. The fluorescence emission spectra were recorded until the fluorescence intensity at the maximum emission wavelength of the

CSP1 protein was completely quenched. The gradient ratio mixture of CSP1/imidacloprid (1:0, 1:1, 1:5, 1:9, and 1:13 μmol L^{-1}) were titrated with 10 mmol L^{-1} β-ionone under the same conditions, respectively. The binding constants of β-ionone with different ratio mixture of CSP1 with imidacloprid were calculated and compared.

3. Results and discussion

3.1. Expression of recombinant CSP1 protein and fluorescence quenching spectra

The plasmid pET-32a (+)/CSP1 was transformed into the competent BL21 (*DE3*) *E. coli*. After induced by IPTG, and purified by Ni^{2+}-NTA column, the recombinant CSP1 protein was obtained through the thorough dialysis in PBS. The result of SDS-PAGE electrophoresis of protein induction and purification was shown in Fig. 1, Lane 1 and lane 2 shows that the whole of lysis bacterial proteins including pET32-CSP1 plasmid without and with induction of 1 mmol L^{-1} IPTG. Lane 3 was the purified recombinant CSP1 protein. The molecular weight of recombinant CSP1 protein is about 28 KD, and the purity reached above 95%.

When imidacloprid was titrated into the recombinant CSP1 protein system, as shown in Fig. 2(A), the fluorescence emission spectra of CSP1 were quenched at the maximum emission wavelength of about 332 nm, with the increase of imidacloprid concentration. It indicated that imidacloprid could regularly quench the intrinsic fluorescence of CSP1 protein. That is, there was an occurrence of the binding interaction between imidacloprid and CSP1.

3.2. Synchronous fluorescence spectra

In order to further study the micro-conformational changes of the two major fluorescent amino acids (Tyrosine and Tryptophan) in CSP1 interacting with imidacloprid, synchronous fluorescence scanning was performed when $\Delta\lambda = 15$ and 60 nm, respectively. Both of the wavelengths reflect the tyrosine and tryptophan residues in the binding site of the fluorescence characteristics, respectively [35]. In addition, the change in the polarity of the protein binding site can be evaluated by the change of the maximum emission wavelength.

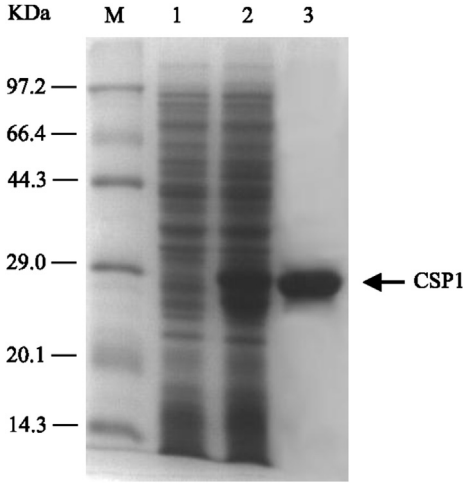

Fig. 1. SDS-PAGE of induced and purified recombinant CSP1 protein. M represents protein molecular weight marker. Lane 1 and lane 2 shows that the whole of lysis bacterial proteins including pET32-CSP1 plasmid without and with induction of 1 mmol L^{-1} IPTG, respectively. Lane 3 shows that the purified recombinant CSP1 protein, which is pointed by a black arrow on the right of the figure.

As shown in Fig. 2(B and C), tryptophan fluorescence intensity was significantly higher than tyrosine, indicating that the fluorescence intensity of CSP1 mainly from tryptophan. With the increase of imidacloprid concentration, tryptophan fluorescence quenching is more intense than tyrosine, suggesting that tryptophan plays a major role in the quenching process and is closer to the binding site. In addition, the maximum emission wavelength of tryptophan produced the red shift Fig. 2(C), indicating that the tryptophan residue of the hydrophobicity of the microenvironment is reduced and the polarity is increased [36]. In contrast, the maximum emission wavelength of tyrosine is essentially constant, so the polarity does not change (Fig. 2(B)). The above shows that tryptophan is mainly involved in the interaction of CSP1 with imidacloprid, which is consistent with other reported chemosensory proteins [37], pheromone binding protein [38], even serum albumin [39], and so on.

3.3. Fluorescence quenching mechanism

Fluorescence quenching due to different mechanisms can be divided into dynamic quenching and static quenching [40]. Dynamic quenching is a quenching phenomenon caused by excitation energy in the excited state, which is the result of molecular collision. Static quenching is caused by the stable complex formed by the ground state fluorescent substance and quencher [41]. Dynamic quenching was performed using the Stern-Volmer equation [42]:

$$\frac{F_0}{F} = 1 + K_q\tau_o[Q] = 1 + K_{sv}[Q] \quad (1)$$

Where F_0 is the fluorescence intensity of the fluorescent material when imidacloprid is not added; F is the fluorescence intensity of the fluorescent substance when the quencher concentration is equal to [Q]; K_q is the fluorescence quenching rate constant; (The average lifetime of the bioprospector is about $\tau_0 = 10^{-8}$ s); K_{sv} is the Stern-Volmer dynamic quenching constant [43]. The fluorescence intensities at 284 and 294 K were measured, respectively. As shown in Fig. 3(A) and Table 1, the K_{sv} value increased with increasing temperature, indicating that the quenching mechanism was dynamic quenching. Since dynamic quenching is produced by molecular diffusion, the higher the temperature, the more intermolecular collisions [44].

The dynamic binding between the protein and the small molecule ligand does not form a complex, and the mixing system will remain stable, which means that the UV absorption spectrum of the protein will remain constant after the addition of the small molecule ligand [45]. As shown in Fig. 3(B), the UV absorption peak shape of CSP1 showed almost no change after addition of imidacloprid in equimolar concentration (1 μmol L^{-1}), indicating that CSP1 did not form a complex with imidacloprid, further confirming its quenching mechanism as dynamic quenching. Interestingly, this dynamic binding of imidacloprid to CSP1 is quite different from the previously reported static binding of imidacloprid to odorant-binding protein ASP2 in *A. cerana* [46], suggesting that the interaction patterns of these two chemoreceptive proteins of insects with imidacloprid are different.

3.4. Thermodynamic analysis

In general, weak interactions between macromolecules and small organic molecules mainly include hydrogen bonds, van der Waals forces, electrostatic interactions and hydrophobic interactions [47]. The above forces are related to the following thermodynamic parameters:

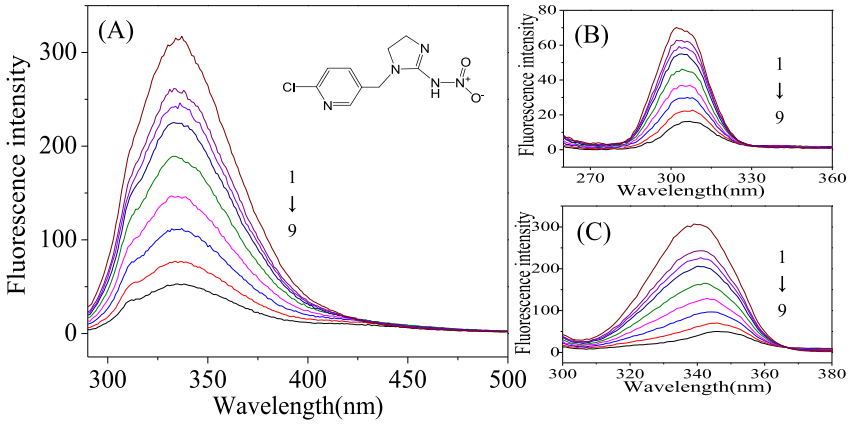

Fig. 2. Fluorescence quenching spectra and chemical structure of imidacloprid (inset) (A) and synchronous fluorescence spectra of CSP1 and imidacloprid (B, C). (A). As imidacloprid titrated in from 1 to 9 (final concentration is 0, 5, 7, 9, 14, 21, 30, 45, and 63 μmol L^{-1}, respectively), the fluorescence intensity of CSP1 obviously decreased. (B): $\Delta\lambda = 15$ nm (tyrosine). When imidacloprid is titrated, the fluorescence intensity of CSP1 also decreases slightly. (C): $\Delta\lambda = 60$ nm (tryptophan). When imidacloprid is titrated, the fluorescence intensity of CSP1 decreases sharply. The maximum emission wavelength has an obvious red shift from 339 to 346 nm. (For interpretation of the references to colour in this figure legend, the reader is referred to the web version of this article.)

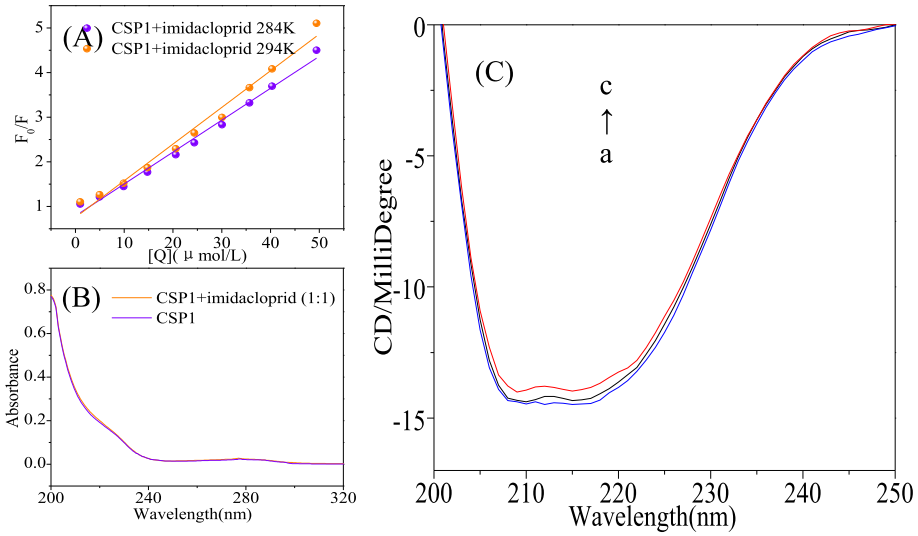

Fig. 3. Dynamic quenching mechanism and circular dichroism (CD) spectra of CSP1 interacting with imidacloprid. (A). The Stern-volmer plots of fluorescence quenching of CSP1 by imidacloprid at 284 K and 294 K. (B). The UV spectral comparison of CSP1 and the mixture of CSP1 and imidacloprid with equal concentration of 1 μmol L^{-1} (C). As imidacloprid added in (final concentration of imidacloprid from a to c is 0, 0.3, 2.7 μmol L^{-1}, respectively), the typical shoulder peaks of CSP1 α-helix increased at 208 and 222 nm.

Table 1
Fluorescence quenching constants (in equation of Stern-Volmer) and the thermodynamic parameters at different temperature.

System	T/K	K_{sv}/(L mol^{-1})	K_q/(L mol^{-1} s^{-1})	ΔH/(KJ mol^{-1})	ΔS/(J mol^{-1} K^{-1})	ΔG/(KJ mol^{-1})	Binding force
CSP1/imidacloprid	284	7.15×10^4	7.15×10^{12}	14.383	138.887	−25.061	Hydrophobic interaction
	294	8.22×10^4	8.22×10^{12}			−26.450	

$$\Delta G = -RT \ln K = \Delta H - T\Delta S \quad (2)$$

$$\Delta H = \frac{RT_1T_2 \ln(K_{0,2}/K_{0,1})}{T_2 - T_1} \quad (3)$$

$$\Delta S = (\Delta H - \Delta G)/T \quad (4)$$

ΔG, ΔH and ΔS are the change of Gibbs free energy, enthalpy change and entropy change, respectively. When $\Delta H < 0$ and $\Delta S < 0$, it is shown that the two functions are based on hydrogen bond and Van der Waals force. When $\Delta H > 0$ and $\Delta S > 0$, the effect is based on the typical hydrophobic interaction. When $\Delta H < 0$ and $\Delta S > 0$, they are generally hydrophobic and electrostatic forces [48]. The thermodynamic parameters of CSP1 and imidacloprid were calculated as shown in Table 1. Since $\Delta G < 0$, the binding between CSP1 and imidacloprid was based on the spontaneous effect of the decrease of free energy. Since $\Delta H > 0$ and $\Delta S > 0$, it is shown that the main driving force of the interaction is hydrophobic force. This hydrophobic interaction is consistent with the interaction between ASP2 and imidacloprid [46], suggesting that imidacloprid has similarity to the action of insects chemoreceptive proteins.

3.5. Circular dichroism (CD) spectra

CD spectroscopy is always used to study the secondary structure change of protein when binding with small molecule ligands [49]. The double negative peaks at 208 and 222 nm are typical CD spectral characteristics of the α-helix structure in the protein [50]. As see in Fig. 3(C), the double negative peaks of CSP1 declined with the increase of imidacloprid concentration, indicating that the binding of imidacloprid resulted in the change of the secondary structure, that is, the extension of peptide chain of CSP1 protein. This is also similar to the interaction of ASP2 and imidacloprid, indicating that the changes of secondary conformation of the two proteins to imidacloprid are similar [46].

3.6. Molecular docking

According to the CSPMbraA6 crystal structure (PDB ID, 1n8v) of *Mamestrabrassicae* [32], the three-dimensional crystal structure of CSP1 was obtained by using the SWISS-MODEL algorithm. The sequence alignment of CSP1 and CSPMbraA6 (1n8v) is shown in Fig. 4(B). According to the MolDock energy score (Table 2), the optimal model for the binding of CSP1 to imidacloprid was estimated and shown in Fig. 3(A). Based on this model, there were 8 major amino acids predicted in the interaction between CSP1 and imidacloprid, including four hydrophobic residues (Val11, Phe43, Phe44, and Ile62), one polar neutral residue (Gln63), 2 acid residues (Asp9 and Asp40), and one basic residue (His47) (Fig. 3(A)). From Fig. 3(A), imidacloprid is also close to the two tryptophan (Trp 73 and Trp82) in CSP1, which is consistent with the results that tryptophan mainly contribute the fluorescence emission in section of CSP1 synchrotron fluorescence spectra (Fig. 3(B)).

Table 2
Individual residue contribution in CSP1 that interacts with imidacloprid.

Residues interacted	Site Number	Epair[a]
Phe	44	−24.1035
Gln	63	−16.0482
Asp	9	−9.4608
Phe	43	−9.3838
Asp	40	−8.6277
His	47	−7.3377
Ile	62	−6.9446
Val	11	−4.0133

[a] Epair: hydrophobic and electrostatic forces energy between a ligand atom and a receptor atom.

3.7. Functional inhibition of CSP1 by imidacloprid

For the further investigation of imidacloprid affecting the function of CSP1 in vitro, 10 mmol L^{-1} β-ionone was titrated with 1 μmol L^{-1} CSP1 protein solution as well as a serious of mixture of imidacloprid and CSP1 protein in different proportions (molar ratio of CSP1: imidacloprid was 1:1, 1:5, 1:9 and 1:13, respectively). When excited at 281 nm, the fluorescence emission spectra and the fluorescence intensity at the maximum emission wavelength of 332 nm were recorded. The apparent binding constant K_A was calculated by the double Log equation below [51]:

$$\lg\frac{F_0 - F}{F} = \lg K_A + n\lg[Q] \quad (5)$$

Where F_0 is the fluorescence intensity of the fluorescent substance when the quencher is not added; F is the fluorescence intensity of the fluorescent substance when the quencher concentration is equal to [Q]; K_A is the apparent binding constant; n is the number of binding sites. According to Fig. 4(C) and Table 3, the apparent

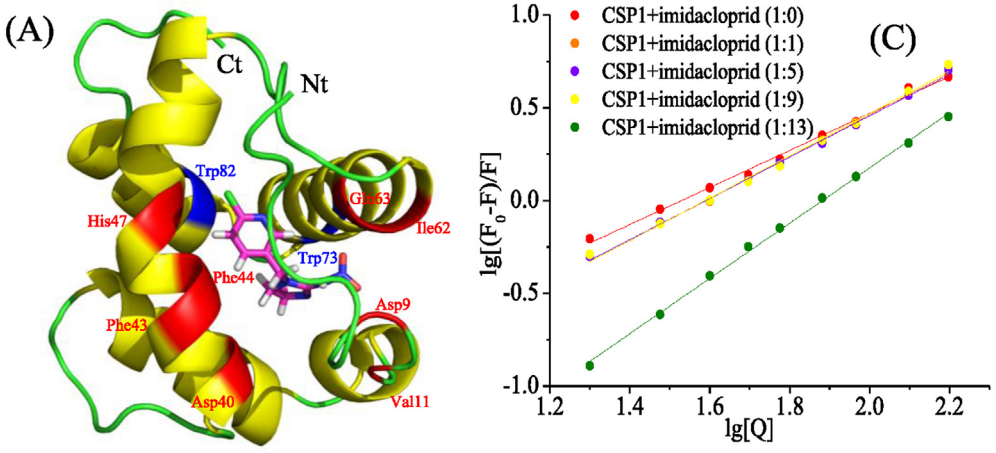

(B)

```
CSP1:      1 EELYSDKYDYVNIDEILANDRLRNQYYDCFIDAGPCLTPDSVFFKSHIT
CSPMbraA6: 1 EDKYTDKYDNINLDEILANKRLLVAYVNCVMERGKC-SPEGKELKEHLQ
CSP1:      EAFQTQCKKCTEIQKQNLDKLAEWFTTNEPEKWNHFVEIMIKKKDEGA 97
CSPMbraA6: DAIENGCKKCTENQEKGAYRVIEHLIKNEIEIWRELTAKYDPTGNW-- 94
```

Fig. 4. Molecular docking of CSP1 with imidacloprid (A) and the Double-Log plots of the fluorescence of the mixture of CSP1 and imidacloprid quenching by β-ionone (C).
(A). Imidacloprid interacts with residues located on α-helices as well as N-terminal flexible region. Red represents the residues that provide hydrophobic interactions. Blue represent tryptophan residues. (B). Amino acid sequence alignment between CSP1 and CSPMbraA6 (1n8v). The 8 residues of CSP1 interacting with imidacloprid are labeled by red letters. Two tryptophan residues are labeled by blue letters. 4 conserved cysteines are shown as yellow shadow. (C). The concentration of CSP1was 1 μmol L^{-1}, and the tittering concentration of β-ionone was 10 mmol L^{-1} (final concentration of imidacloprid is 0, 1, 5, 9, and 13 μmol L^{-1}, respectively. The final concentration of β-ionone is 20, 30, 40, 50, 60, 76, 93, 125 and 157 μmol L^{-1}, in turn). (For interpretation of the references to colour in this figure legend, the reader is referred to the web version of this article.)

Table 3
Fluorescence quenching constants (in equation of Double-Log) of binding interactions of CSP1 with β-ionone, and the complex of CSP1-imidacloprid with different ratio binding with β-ionone.

Complex of binding items	K_A/(L mol^{-1})	n	R^2	Decline %	Sublethal dose (ng/bee)
CSP1+ imidacloprid (1:0)	2.972×10^4	0.9981	0.9946	–	–
CSP1+ imidacloprid (1:1)	1.595×10^4	1.1294	0.9962	46.33	0.28
CSP1+ imidacloprid (1:5)	1.706×10^4	1.1120	0.9977	42.60	1.41
CSP1+ imidacloprid (1:9)	1.543×10^4	1.1405	0.9949	48.08	2.53
CSP1+ imidacloprid (1:13)	0.157×10^4	1.4899	0.9984	94.72	3.75

binding constant $K_{A\ (1:\ 0)}$ of β-ionone and CSP1 is 2.972×10^4 L mol^{-1}, while the molar ratio of CSP1 to imidacloprid is shown as two stages, one is in the case of molar ratio of 1: 1, 1: 5 and 1: 9, the apparent binding constant $K_{A\ (1:\ 1\sim9)} = 1.543-1.706 \times 10^4$ L mol^{-1}, decreased by 42.6–48.08% compared with $K_{A\ (1:\ 0)}$; another is in the case of molar ratio of 1: 13, the apparent binding constant $K_{A\ (1:\ 13)} = 0.157 \times 10^4$ L mol^{-1}, decreased by 94.7% compared with $K_{A\ (1:\ 0)}$. According to the quantitative results of the CSP1 protein in the worker bee antennal proteome [52], it is possible to inhibit the binding of CSP1 to β-ionone by nearly 50% in the presence of 0.28–2.53 ng/bee of imidacloprid, however at 3.75 ng/bee, the inhibition rate of even nearly 95%. Since the sublethal dose (RC_{50}) of the imidacloprid to the bee was about 0.15–6.0 ng (95% CI 5.1–9.0 ng) [53,54]. Compared to imidacloprid inhibited the binding of ASP2 to natural ligand by about 26% [46], the inhibitory of imidacloprid effect on CSP1 was significantly stronger. Therefore, it was confirmed that the molecular mechanism of chemoreceptive system of bees was still inhibited by imidacloprid at the sublethal dose level, and the functional inhibition of imidacloprid on CSP1 also was related to the dosage in a unique way.

4. Conclusion

In summary, the neonicotinoid imidacloprid can produce spontaneous binding interaction with CSP1 protein in *A. cerana*, and the quenching mechanism is dynamic quenching. Simultaneous fluorescence experiments showed that tryptophan played a major role in CSP1 fluorescence quenching. Thermodynamic results confirmed that the main force between them was hydrophobic, and the molecular docking predicted the binding pose between them. Circular dichroism (CD) spectra indicated that imidacloprid could change the secondary structure of CSP1 to natural ligand β-ionone. Finally, it was confirmed that imidacloprid at the sublethal dose could significantly inhibit the binding ability of CSP1 to natural ligand β-ionone.

Conflict of interest statement

We declare that we have no conflict of interest.

Acknowledgements

This work was supported by the National Natural Science Foundation of China (No. 31372254, 31672498), the Earmarked Fund for Modern Agro-industry Technology Research System from the Ministry of Agriculture of China (CARS-45) and the Agricultural Public Project of Jinhua City (No. 2016-4-001).

References

[1] J. Pettersson, Foraging in a complex environment - semiochemicals support searching behaviour of the seven spot ladybird. A review, Eur. J. Entomol. 102 (2005) 365–370.
[2] P. Pelosi, J.J. Zhou, L.P. Ban, M. Calvello, Soluble proteins in insect chemical communication, Cell Mol. Life Sci. 63 (2006) 1658–1676.
[3] P. Pelosi, I. Iovinella, A. Felicioli, F.R. Dani, Soluble proteins of chemical communication: an overview across arthropods, Front. physiol. 5 (2014) 320.
[4] A. Nomura, K. Kawasaki, T. Kubo, S. Natori, Purification and localization of p10, a novel protein that increases in nymphal regenerating legs of *Periplaneta americana* (American cockroach), Int. J. Dev. Biol. 36 (1992) 391–398.
[5] J. Maleszka, S. Forêt, R. Saint, R. Maleszka, RNAi-induced phenotypes suggest a novel role for a chemosensory protein CSP5 in the development of embryonic integument in the honeybee (*Apis mellifera*), Dev. Genes & Evol. 217 (2007) 189–196.
[6] W. Guo, X. Wang, Z. Ma, L. Xue, J. Han, D. Yu, L. Kang, CSP and takeout genes modulate the switch between attraction and repulsion during behavioral phase change in the migratory locust, PLoS Genet. 7 (2011) e1001291.
[7] S.H. Gu, S.Y. Wang, X.Y. Zhang, P. Ji, J.T. Liu, G.R. Wang, K.M. Wu, Y.Y. Guo, J.J. Zhou, Y.J. Zhang, Functional characterizations of chemosensory proteins of the alfalfa plant bug *Adelphocoris lineolatus* indicate their involvement in host recognition, PLoS One 7 (2012) e42871.
[8] L. Sun, J.J. Zhou, S.H. Gu, H.J. Xiao, Y.Y. Guo, Z.W. Liu, Y.J. Zhang, Chemosensillum immunolocalization and ligand specificity of chemosensory proteins in the alfalfa plant bug *Adelphocoris lineolatus* (Goeze), Sci. Rep. 5 (2015).
[9] Z.K. Zhang, Z.R. Lei, Identification, expression profiling and fluorescence-based binding assays of a chemosensory protein gene from the Western flower thrips, *Frankliniella occidentalis*, PLoS One 10 (2015) e0117726.
[10] F. Wu, X.M. Zhang, L. Zhao, X.H. Cui, H.L. Li, C. Luo, Binding characterization of chemosensory protein CSP1 in the *Bemisia tabaci* Biotype Q with plant volatiles, Sci. Agric. Sin. 48 (2015) 1955–1961.
[11] S. Angeli, F. Ceron, A. Scaloni, M. Monti, G. Monteforti, A. Minnocci, R. Petacchi, P. Pelosi, Purification, structural characterization, cloning and immunocytochemical localization of chemoreception proteins from *Schistocerca gregaria*, Eur. J. Biochem. 262 (1999) 745–754.
[12] G. Monteforti, S. Angeli, R. Petacchi, A. Minnocci, Ultrastructural characterization of antennal sensilla and immunocytochemical localization of a chemosensory protein in *Carausius morosus* Brünner (Phasmida: Phasmatidae), Arthropod Struct. Dev. 30 (2002) 195–205.
[13] L. Briand, N. Swasdipan, C. Nespoulous, V. Bezirard, F. Blon, J.C. Huet, P. Ebert, J.C. Penollet, Characterization of a chemosensory protein (ASP3c) from honeybee (*Apis mellifera* L.) as a brood pheromone carrier, Eur. J. Biochem. 269 (2002) 4586–4596.
[14] M. Ozaki, A. Wada-Katsumata, K. Fujikawa, M. Iwasaki, F. Yokohari, Y. Satoji, T. Nisimura, R. Yamaoka, Ant nestmate and non-nestmate discrimination by a chemosensory sensillum, Science 309 (2005) 311–314.
[15] J.E. Jepson, L.A. Brown, D.B. Sattelle, The actions of the neonicotinoid imidacloprid on cholinergic neurons of *Drosophila melanogaster*, Invertebr. *Neurosci.* 6 (2006) 33–40.
[16] J.E. Casida, K.A. Durkin, Neuroactive insecticides: targets, selectivity, resistance, and secondary effects, Annu. Rev. Entomol. 58 (2013) 99–117.
[17] D. Laurino, A. Manino, A. Patetta, M. Porporato, Toxicity of neonicotinoid insecticides on different honey bee genotypes, Bull. Insectol. 66 (2013) 119–126.
[18] N. Desneux, A. Decourtye, J.M. Delpuech, The sublethal effects of pesticides on beneficial arthropods, Annu. Rev. Entomol. 52 (2007) 81–106.
[19] J. Bryden, R.J. Gill, R.A. Mitton, N.E. Raine, V.A. Jansen, Chronic sublethal stress causes bee colony failure, Ecol. Lett. 16 (2013) 1463–1469.
[20] J. Wu-Smart, M. Spivak, Sub-lethal effects of dietary neonicotinoid insecticide exposure on honey bee queen fecundity and colony development, Sci. Rep. 6 (2016) 32108.
[21] M.A.M. Bautista, B. Bhandary, A.J. Wijeratne, A.P. Michel, C.W. Hoy, O. Mittapalli, Evidence for trade-offs in detoxification and chemosensation gene signatures in *Plutella xylostella*, Pest Manag. Sci. 71 (2015) 423.
[22] N. Xuan, X. Guo, H.Y. Xie, Q.N. Lou, X.B. Lu, G.X. Liu, J.F. Picimbon, Increased expression of CSP and CYP genes in adult silkworm females exposed to avermectins, Insect Sci. 22 (2015) 203–219.
[23] G. Liu, H. Ma, H. Xie, X. Ning, X. Guo, Z. Fan, B. Rajashekar, P. Arnaud, B. Offmann, J.F. Picimbon, Biotype characterization, developmental profiling, insecticide response and binding property of *Bemisia tabaci* chemosensory proteins: role of CSP in insect defense, PLoS One 11 (2016) e0154706.
[24] D. Park, J.W. Jung, B.S. Choi, M. Jayakodi, J. Lee, J. Lim, Y. Yu, Y.S. Choi, M.L. Lee, Y. Park, Uncovering the novel characteristics of Asian honey bee, *Apis cerana*, by whole genome sequencing, BMC Genomics 16 (2015) 1.
[25] H.L. Li, C.X. Ni, J. Tan, L.Y. Zhang, F.L. Hu, Chemosensory proteins of the eastern honeybee, *Apis cerana*: identification, tissue distribution and olfactory related

functional characterization, Comp. Biochem. Phys. B 194–195 (2016) 11–19.
[26] E.-C. Yang, H.-C. Chang, W.-Y. Wu, Y.-W. Chen, Impaired olfactory associative behavior of honeybee workers due to contamination of imidacloprid in the larval stage, PLoS One 7 (2012) e49472.
[27] S.M. Williamson, G.A. Wright, Exposure to multiple cholinergic pesticides impairs olfactory learning and memory in honeybees, J. Exp. Biol. 216 (2013) 1799–1807.
[28] K. Tan, W. Chen, S. Dong, X. Liu, Y. Wang, J.C. Nieh, Imidacloprid alters foraging and decreases bee avoidance of predators, PLoS one 9 (2014) e102725.
[29] H.L. Li, C.X. Ni, R. Yao, Q.K. Gao, H.W. Shang, Molecular cloning, characterization, and expression pattern of chemosensory protein 1 gene (*Acer-CSP1*) in the Chinese honeybee, *Apis cerana cerana* (Hymenoptera: Apidae), Acta Entomol. Sin. 53 (2010) 962–968.
[30] N. Sreerama, R.W. Woody, Estimation of protein secondary structure from circular dichroism spectra: comparison of CONTIN, SELCON, and CDSSTR methods with an expanded reference set, Anal. Biochem. 287 (2000) 252–260.
[31] W.J. Hu, L. Yan, D. Park, H.O. Jeong, H.Y. Chung, J.M. Yang, Z.M. Ye, G.Y. Qian, Kinetic, structural and molecular docking studies on the inhibition of tyrosinase induced by arabinose, Int. J. Biol. Macromol. 50 (2012) 694–700.
[32] V. Campanacci, A. Lartigue, B.M. Hällberg, T.A. Jones, M.T. Giudiciorticoni, M. Tegoni, C. Cambillau, Moth chemosensory protein exhibits drastic conformational changes and cooperativity on ligand binding, Proc. Natl. Acad. Sci. U. S. A. 100 (2003) 5069–5074.
[33] T. Schwede, J. Kopp, N. Guex, M.C. Peitsch, SWISS-MODEL: an automated protein homology-modeling server, Nucleic acids Res. 31 (2003) 3381–3385.
[34] T. René, M.H. Christensen, MolDock: a new technique for high-accuracy molecular docking, J. Med. Chem. 49 (2006) 3315–3321.
[35] G. Zhang, Q. Que, J. Pan, J. Guo, Study of the interaction between icariin and human serum albumin by fluorescence spectroscopy, J. Mol. Struct. 881 (2008) 132–138.
[36] J.T. Vivian, P.R. Callis, Mechanisms of tryptophan fluorescence shifts in proteins, Biophysical J. 80 (2001) 2093–2109.
[37] H.L. Li, L.Y. Zhang, C.X. Ni, H.W. Shang, S.L. Zhuang, J.K. Li, Molecular recognition of floral volatile with two olfactory related proteins in the Eeastern honeybee (*Apis cerana*), Int. J. Biol. Macromol. 56 (2013) 114–121.
[38] C. Weng, Y.X. Fu, H.T. Jiang, S.L. Zhuang, H.L. Li, Binding interaction between a queen pheromone component HOB and pheromone binding protein ASP1 of *Apis cerana*, Int. J. Biol. Macromol. 72 (2015) 430–436.
[39] H. Li, F. Wu, J. Tan, K. Wang, C. Zhang, H. Zheng, F. Hu, Caffeic acid phenethyl ester exhibiting distinctive binding interaction with human serum albumin implies the pharmacokinetic basis of propolis bioactive components, J. Pharm. Biomed. Analysis 122 (2016) 21–28.
[40] S. Ranjbar, Y. Shokoohinia, S. Ghobadi, N. Bijari, S. Gholamzadeh, N. Moradi, M.R. Ashrafi-Kooshk, A. Aghaei, R. Khodarahmi, Studies of the interaction between isoimperatorin and human serum albumin by multispectroscopic method: identification of possible binding site of the compound using esterase activity of the protein, Sci. World J. 2013 (2013) 205081.
[41] J. Xu, Z. Wang, Methods of Fluorescence Analysis, third ed., Science Press, Beijing, 2006, p. 67.
[42] J.R. Lakowicz, Principles of Fluorescence Spectroscopy, Springer Science & Business Media, 2013.
[43] J.R. Lakowicz, G. Weber, Quenching of protein fluorescence by oxygen. Detection of structural fluctuations in proteins on the nanosecond time scale, Biochemistry 12 (1973) 4171–4179.
[44] W.R. Ware, Oxygen quenchig of fluorescence in solution: an experimental study of the diffusion process, J. Phys. Chem. 66 (1962).
[45] J. Karolin, L. Johansson, L. Strandberg, T. Ny, Fluorescence and absorption spectroscopic properties of dipyrrometheneboron difluoride (BODIPY) derivatives in liquids, lipid membranes, and proteins, J. Am. Chem. Soc. 116 (1994) 7801–7806.
[46] H. Li, F. Wu, L. Zhao, J. Tan, H. Jiang, F. Hu, Neonicotinoid insecticide interact with honeybee odorant-binding protein: implication for olfactory dysfunction, Int. J. Biol. Macromol. 81 (2015) 624–630.
[47] Y.J. Hu, Y. Liu, L.X. Zhang, R.M. Zhao, S.S. Qu, Studies of interaction between colchicine and bovine serum albumin by fluorescence quenching method, J. Mol. Struct. 750 (2005) 174–178.
[48] P.D. Ross, S. Subramanian, Thermodynamics of protein association reactions: forces contributing to stability, Biochemistry 20 (1981) 3096–3102.
[49] N.J. Greenfield, Using circular dichroism spectra to estimate protein secondary structure, Nat. Protoc. 1 (2006) 2876–2890.
[50] B. Yélamos, E. Núñez, M. Datta, B. Pacheco, D.L. Peterson, F. Gavilanes, Circular dichroism and fluorescence spectroscopic properties of the major core protein of feline immunodeficiency virus and its tryptophan mutants, Eur. J. Biochem. 266 (1999) 1081–1089.
[51] L. Zhang, F. Jin, T. Zhang, L. Zhang, J. Xing, Structural influence of graft and block polycations on the adsorption of BSA, Int. J. Biol. Macromol. 85 (2016) 252–257.
[52] D. Woltedji, F. Song, L. Zhang, A. Gala, B. Han, M. Feng, Y. Fang, J. Li, Western honeybee drones and workers (*Apis mellifera ligustica*) have different olfactory mechanisms than eastern honeybees (*Apis cerana cerana*), J. Proteome Res. 11 (2012) 4526–4540.
[53] J.E. Cresswell, A meta-analysis of experiments testing the effects of a neonicotinoid insecticide (imidacloprid) on honey bees, Ecotoxicology 20 (2011) 149–157.
[54] C.W. Schneider, J. Tautz, B. Grunewald, S. Fuchs, RFID tracking of sublethal effects of two neonicotinoid insecticides on the foraging behavior of *Apis mellifera*, PLoS One 7 (2012) e30023.